

# Vibrational mode and collision energy effects on proton transfer in phenol cation–methylamine collisions

Ho-Tae Kim, Richard J. Green, and Scott L. Anderson<sup>a)</sup>

Department of Chemistry, University of Utah, 315 S. 1400 E. Rm 2020, Salt Lake City, Utah 84112-0850

(Received 28 January 2000; accepted 29 March 2000)

Mass-analyzed threshold ionization has been used to prepare vibrationally state-selected phenol cations, that were then reacted with methylamine at collision energies ranging from 0.1 to 2 eV. Integral cross sections and product recoil velocity distributions are reported. *Ab initio* calculations of stationary points on the surface and RRKM (Rice–Ramsperger–Kassel–Marcus) analysis of complex lifetimes are also presented for comparison. The only reaction observed over the entire energy range is exoergic proton transfer (PT). For ground-state reactants, the PT cross section is reduced by increasing collision energy, such that the reaction efficiency declines from  $\sim 71\%$  at low  $E_{\text{collision}}$  to  $\sim 50\%$  at 2 eV. Excitation of either  $\nu_{6a}$  or  $\nu_{12}$  vibrations inhibits reaction over the entire collision energy range, with the effect being somewhat mode-specific and increasing with increasing  $E_{\text{collision}}$ . At low  $E_{\text{collision}}$ , both vibrational and collision energy inhibit reaction with similar efficiency. Collision energy effects diminish at high  $E_{\text{collision}}$ , while vibration continues to have a strong effect. Product ion velocity distributions are approximately forward–backward symmetric at  $E_{\text{collision}} \leq 1$  eV, but are backward peaked at high energies. Mechanistic implications of these results are discussed. © 2000 American Institute of Physics. [S0021-9606(00)00724-8]

## I. INTRODUCTION

Measurements of vibrational effects on reactions of diatomic or small polyatomic molecules have proven to be a useful tool in probing reaction mechanisms, typically providing insight into the nature of the transition state(s) controlling reaction. We have found the combination of mode-selective reactant preparation with measurements of product recoil velocity distributions to be a particularly powerful tool in the study of ion–molecule reaction dynamics. Thus far, only three to four atom polyatomic ions have been subjected to this type of experiment, largely because preparation of mode-selectively excited polyatomic reactant ions is a difficult proposition.<sup>1</sup> Zare and co-workers have used single-color REMPI (resonance-enhanced multiphoton ionization) to study state-selected reactions of  $\text{NH}_3^+$ ,<sup>2–4</sup> and for several diatomic cations. Using REMPI, we have probed reactions of  $\text{OCS}^+$ ,<sup>5–8</sup>  $\text{C}_2\text{H}_2^+$ ,<sup>7,9–14</sup> and  $\text{NH}_3^+$ .<sup>15</sup> Threshold photoelectron–photoion coincidence has been used by Duit, Guyon, and co-workers,<sup>16,17</sup> and by Koyano and co-workers<sup>18–20</sup> for state selected studies of atomic, diatomic, and acetylene cation reactions. Little or nothing is known about the effect of vibrational excitation on reaction of significantly larger cations. This letter reports a study of the reaction of phenol cation with methylamine (MA), in which mass analyzed threshold ionization (MATI)<sup>21</sup> was used to prepare  $\text{C}_6\text{H}_5\text{OH}^+$  in selected vibrational states.

One reason for interest in the  $\text{PhOH}^+ + \text{MA}$  reaction is for comparison with the  $\text{PhOH}^+ + \text{ND}_3$  reaction. In that system, we find that proton transfer (PT) is a minor channel, with the dominant reaction being *H/D* exchange, mediated

by a long-lived intermediate complex.<sup>22</sup> The small PT probability was unexpected, as *ab initio* calculations<sup>22,23</sup> indicate that there is no barrier to intracomplex PT, and the literature<sup>24,25</sup> suggested that the PT and *H/D* exchange reactions are nearly isoenergetic. Our conclusion, based on RRKM simulations of the energy dependence of the product branching ratio was that the PT reaction is actually 0.20 eV endoergic. In drawing this conclusion we assumed that, other than the endoergicity, there is no significant barrier or dynamical bottleneck to PT. In this context, the  $\text{PhOH}^+ + \text{MA}$  system is interesting in that the PT mechanism is presumably similar to that for  $\text{ND}_3$ , but PT is clearly exothermic (0.44 eV).<sup>24,25</sup> If a dynamical bottleneck or significant barrier existed along the  $\text{PhOH}^+ + \text{ND}_3$  PT coordinate, we might expect to see some sign in the results for  $\text{PhOH}^+ + \text{MA}$  as well. As noted below, comparison of the two systems also suggests a common, rather unusual vibrational effect on PT.

## II. EXPERIMENT

Reactions were studied in a guided-ion beam instrument that has been described previously,<sup>7,13</sup> along with the methodologies used in the experiments and data analysis. Vibrationally state-selected  $\text{PhOH}^+$  was prepared by MATI of a pulsed beam of phenol seeded in helium. Phenol was single-photon excited to a particular vibrational level of the  $^1L_b(S_1)$  state, then excited with a second laser to high Rydberg states converging on the same vibration in the cation. Prompt ions created by REMPI, autoionization, or other processes were separated from the state-selected Rydberg molecules by a weak retarding field ( $\sim 3$  V/cm). After a time delay of  $\sim 6$   $\mu\text{s}$ , the Rydberg molecules were field-ionized by a 30 V/cm pulse, creating a beam of state-selected reactant ions.

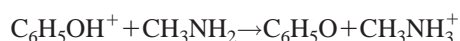
<sup>a)</sup>Electronic mail: anderson@chemistry.utah.edu

Three vibrational states were studied—the ground state, a state with one quantum of a  $516\text{ cm}^{-1}$  vibration, and a state with one quantum of an  $815\text{ cm}^{-1}$  vibration. The vibrations are assigned as  $\nu_{6a}$  and  $\nu_{12}$ , respectively, based on earlier MPI (multiphoton ionization) photoelectron spectroscopy<sup>26</sup> and our *ab initio* calculations (see below). These are both in-plane ring deformations, involving some motion of the OH group as a unit, but with no OH stretching character. High-energy vibrations, including the OH stretch, are, unfortunately, not selectable because rapid IVR in the intermediate and/or Rydberg electronic states makes MATI production of sufficient intensities impossible. The low-frequency modes studied are stable with respect to IVR, simply because there are no near-degenerate combinations of lower frequency modes with the correct symmetry.

The ion beam was injected into a quadrupole ion guide that focused the ions on an exit aperture/lens system. Using a combination of the quadrupole's focusing properties<sup>27</sup> and time-of-flight (TOF) gating at the quadrupole exit lens, non-MATI ions were rejected and the temporal width of the beam pulse was narrowed to  $\sim 15\ \mu\text{s}$ . The beam was then injected into an octapole ion guide system, and passed through a scattering cell containing  $6 \times 10^{-5}$  Torr of methylamine vapor. Product ions, together with unreacted  $\text{PhOH}^+$ , were collected by the ion guide and conveyed to a quadrupole mass filter for analysis. The ion guide is divided into two segments, with the joint just after the scattering cell. This allows us to accelerate the ions immediately following their exit from the scattering cell, improving collection for slow product ions. TOF was used to record both reactant and product velocity distributions. Methylamine (Matheson, 99.5%) was used without purification, and its pressure in the scattering cell was adjusted to maintain single collision conditions, as shown by the pressure-independence of the measured cross sections.

### III. RESULTS AND DISCUSSION

Several reactions are possible<sup>24,25</sup> in our energy range



$$\Delta H = -0.437\text{ eV}$$



Only proton transfer (PT) is observed to be significant, and the cross sections are shown in Fig. 1 over the center-of-mass energy range from 0 to 2 eV. The main graph gives cross sections as a function of collision energy. The inset re-plots the data as a function of total energy ( $= E_{\text{collision}} + E_{\text{vibration}}$ ). Note that from experiments with  $\text{C}_6\text{D}_5\text{OH}^+$ , we can rule out involvement of the phenyl hydrogen atoms in the PT chemistry.

To give some idea of the type of vibrational motion excited, the extrema of trajectories for each normal mode are superimposed at the top of Fig. 1. Normal coordinates are from GAUSSIAN 98 calculations<sup>28</sup> (see below), visualized using GOPENMOL.<sup>29</sup> Note that neither mode involves OH stretching.  $\nu_{6a}$  involves collective motion of the COH moi-

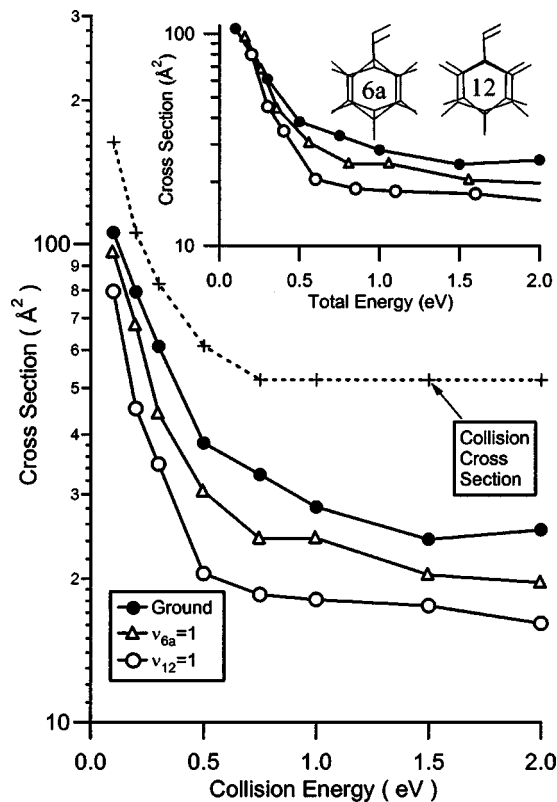


FIG. 1. Main figure: Cross sections for proton transfer from  $\text{PhOH}^+$  to methylamine as a function of collision energy, for different  $\text{PhOH}^+$  vibrational states. Also shown is an estimate of the collision cross section. Inset: Cross sections as a function of total energy. Also shown are superimposed plots of the vibrational extrema for the two vibrations excited.

ety, with little change in CO bond length or COH bond angle.  $\nu_{12}$  also preserves the COH angle, but has significant CO stretching character.

Also shown in Fig. 1 is an estimate of the collision cross section, taken as the greater of the capture cross section (low energies)<sup>30</sup> and the hard-sphere cross section (high energies). We can define the reaction efficiency as the ratio of the experimental PT cross section to the collision cross section. For ground-state  $\text{PhOH}^+$ , the efficiency is  $\sim 71\%$  at low  $E_{\text{collision}}$ , dropping slowly to  $\sim 50\%$  at high  $E_{\text{collision}}$ . The effect of  $\text{PhOH}^+$   $\nu_{6a}$  excitation ( $516\text{ cm}^{-1}$ ) is to decrease the cross section (and efficiency) by  $17\%$ – $20\%$ , relative to the ground state, the effect being slightly larger at high  $E_{\text{collision}}$ . The effect of  $\nu_{12}$  excitation ( $815\text{ cm}^{-1}$ ) is larger—a  $\sim 37\%$  inhibition at low  $E_{\text{collision}}$  increasing to a  $\sim 43\%$  inhibition at high  $E_{\text{collision}}$ . At low  $E_{\text{collision}}$ , the effects of vibration and collision energy are similar (see  $\sigma$  vs  $E_{\text{total}}$  inset in Fig. 1) indicating that total energy, rather than a particular form of energy, is responsible for suppressing reactivity. At high  $E_{\text{total}}$  the cross sections are nearly independent of collision energy, while the inhibitory effects of vibrational excitation actually increase slightly at higher energies. At high energies the vibrational effect is also mode-specific, i.e.,  $\nu_{12}$  gives  $\sim 35\%$  larger inhibition than would be expected from scaling the  $\nu_{6a}$  effect by the ratio of the vibrational energies.<sup>13</sup>

Figure 2 shows lab-frame axial velocity distributions<sup>13</sup> for the protonated MA product. The heavy vertical lines

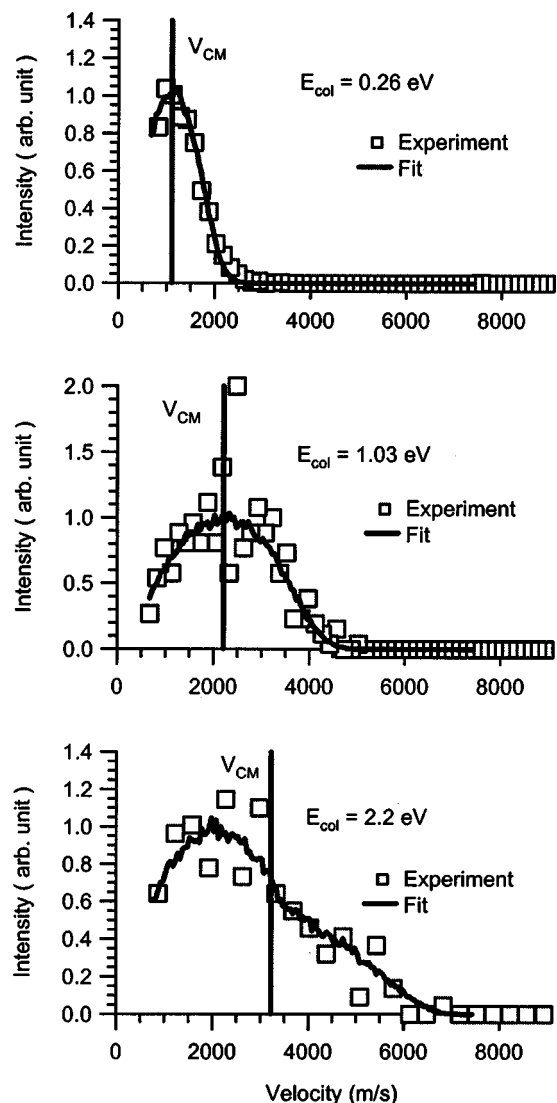


FIG. 2.  $\text{HMA}^+$  product lab frame axial recoil velocity distributions.  $V_{\text{CM}}$  is shown as a heavy vertical line in each frame.

show the velocity of the center-of-mass (cm) ( $V_{\text{CM}}$ ) in the lab frame. Axial velocity distributions are the projection of the full distribution on the octapole axis, which is co-axial with the average relative velocity vector for the collisions. Note that small potential inhomogeneities in the octapoles tend to result in loss or velocity distortions for ions with low lab-frame velocities. For this reason, only the velocity range above 600 m/s ( $\sim 60$  meV lab energy) is plotted.

The velocity distributions provide two, related pieces of information. The maximum deviation of the velocity distribution from  $V_{\text{CM}}$  is a measure of the maximum energy going into recoil of the products. If reaction proceeds via a collision intermediate with lifetime long compared to its rotational period (see below), the distributions are forward-backward symmetric with respect to  $V_{\text{CM}}$ . Conversely, an asymmetric velocity distribution is the signature of a direct reaction where the collision time is short. For the PT reaction, the distributions are forward-backward symmetric within experimental error for  $E_{\text{collision}}$  up to  $\sim 1$  eV, then become backward-peaked at high energies. Note that the dis-

tributions also become substantially wider as  $E_{\text{collision}}$  is raised, indicating higher recoil energy. Both forward-backward symmetry and low  $E_{\text{recoil}}$  suggest that the mechanism at low  $E_{\text{collision}}$  involves a complex, with a transition to direct scattering at high energies.

In this scenario, it is reasonable to fit the distributions using the osculating complex model of Fisk *et al.*<sup>31</sup> Fitting allows us to correct for the effects of experimental broadening factors (e.g., reactant velocity distributions) and to estimate both the complex lifetime and the recoil energy distribution. Fitting is done with a Monte Carlo simulation of the experiment, as discussed previously.<sup>13</sup> In the osculating complex model a complex is assumed to form, decomposing to products unimolecularly with lifetime,  $\tau_{\text{complex}}$ . The complex also rotates, with classical rotational period,  $\tau_{\text{rotation}}$ , determined by its moment of inertia and the available angular momentum, which may be estimated from the magnitude of the cross section and collision energy. For the  $\text{PhOH}^+ - \text{MA}$  system,  $\tau_{\text{rotation}}$  drops smoothly from  $\sim 3$  ps at  $E_{\text{collision}} = 0.1$  eV to  $\sim 1.3$  ps at 2 eV. If  $T_{\text{Ratio}} = \tau_{\text{rotation}} / \tau_{\text{complex}}$  is much greater than 1, then products will be distributed isotropically in the scattering plane of each collision, giving rise to an axial velocity distribution that is forward-backward symmetric with respect to  $V_{\text{CM}}$ . As  $\tau_{\text{complex}}$  drops below  $\sim 0.5 \tau_{\text{rotation}}$ , noticeable asymmetry with respect to  $V_{\text{CM}}$  may become apparent, providing a signature for decreasing collision time. In our fitting, the recoil energy distribution is assumed to be a Gaussian peaking at  $f_{\text{peak}} \cdot E_{\text{avail}}$  with width  $= f_{\text{width}} / E_{\text{avail}}$ :

$$P(E_{\text{recoil}}) = \exp - \left( \frac{f_{\text{width}} \cdot [E_{\text{recoil}} - f_{\text{peak}} \cdot E_{\text{avail}}]}{E_{\text{avail}}} \right)^2.$$

The fits depend on only three parameters ( $T_{\text{Ratio}}$ ,  $f_{\text{width}}$ ,  $f_{\text{peak}}$ ), all of which are physically significant.

Osculating complex fits to the data are shown as curves in Fig. 2, and the results are as follows. At collision energies up to 1 eV,  $\tau_{\text{complex}}$  is greater than  $\tau_{\text{rotation}}$ , which varies from  $\sim 3$  to  $\sim 1.7$  ps over this energy range. At  $E_{\text{collision}} = 2.2$  eV,  $\tau_{\text{complex}}$  drops to  $\sim 22\%$  of the rotational period, or  $\sim 290$  fs. The  $E_{\text{recoil}}$  distribution,  $P(E_{\text{recoil}})$ , provides further evidence for a decrease in collision complex lifetime with increasing energy. At  $E_{\text{collision}} = 0.26$  eV,  $P(E_{\text{recoil}})$  peaks at zero, with mean  $E_{\text{recoil}} \approx 12\%$  of the available energy ( $E_{\text{avail}} = E_{\text{collision}} + E_{\text{vibration}} + \text{exoergicity}$ ). This result is consistent with a complex in which extensive redistribution of the available energy occurs. Note that equipartition among all active modes of the complex, i.e., modes with energy  $\leq E_{\text{avail}} / (\# \text{active modes})$  would give  $\langle E_{\text{recoil}} \rangle \approx 8\% \cdot E_{\text{avail}}$ . At  $E_{\text{collision}} = 1.03$  eV,  $P(E_{\text{recoil}})$  still peaks at zero, but is broadened such that  $\langle E_{\text{recoil}} \rangle \approx 25\% E_{\text{avail}}$ , as opposed to  $\sim 7\%$  for equipartition among all modes active at this available energy. The increase in  $E_{\text{recoil}} / E_{\text{avail}}$  suggests less time for energy redistribution, but note that  $\tau_{\text{complex}}$  is still  $\geq \sim 1$  ps. Finally, at 2.2 eV, it is no longer possible to fit the data with  $P(E_{\text{recoil}})$  peaking at zero. The best fit  $E_{\text{recoil}}$  distribution peaks at 30% of  $E_{\text{avail}}$ , and is somewhat narrower than the distributions at lower  $E_{\text{collision}}$ , both changes being consistent with less time for energy redistribution. At 2.2 eV,  $\langle E_{\text{recoil}} \rangle$  is  $\sim 38\%$  of  $E_{\text{avail}}$  (compared to  $\sim 5\%$  for equipartition among

active modes), and  $\tau_{\text{complex}} \approx 290$  fs. Note that the osculating complex analysis assumes that the angular distribution is entirely the result of rotation of the complex, whereas in reality, the inherent scattering dynamics will result in some angular spread. As a result, the 290 fs  $\tau_{\text{complex}}$  should be regarded as an upper limit on the collision time. Note also that the back-scattered HMA<sup>+</sup> product observed at high energies corresponds to transfer of the proton between PhO and MA moieties that continue in their original directions (i.e., ‘stripping’). It is clear from the broad velocity distribution, however, that the dynamics are far from the spectator stripping limit, and that there is substantial momentum transfer in the collisions. (True spectator stripping would give a sharp peak at 130 m/s in the lab frame.)

To aid interpretation of the results, we have calculated the stationary point energetics of this system at the B3LYP/6-31G\* level (including zero-point energy correction) using GAUSSIAN 98.<sup>28</sup> The proton transfer exoergicity is calculated to be 0.45 eV, in excellent agreement with the literature energetics (0.44 eV),<sup>25</sup> suggesting that this level of theory is adequate for our purposes. We located a hydrogen-bonded complex with phenoxy-protonated-MA structure (PhO–HMA<sup>+</sup>). This productlike complex is 1.69 eV below the reactant energy, and is bound by 1.25 eV with respect to products. We also attempted to find a hydrogen-bonded, reactantlike complex (PhOH–MA)<sup>+</sup>, however, this starting geometry optimized to the productlike complex (PhO–HMA)<sup>+</sup>, indicating no barrier to intracomplex proton transfer. Absence of a barrier is unsurprising, considering that there is no significant barrier in the (PhOH–NH<sub>3</sub>)<sup>+</sup> system,<sup>22,23</sup> and that the proton affinity of MA is  $\sim 0.6$  eV greater than that of ammonia.

In addition to the hydrogen-bonded, productlike complex (PhO–HMA<sup>+</sup>), we optimized several nonhydrogen-bonded, reactantlike complexes. The most stable has MA positioned such that its nitrogen lone pair orbital is pointing at the para carbon atom in PhOH<sup>+</sup>, with the lone pair axis nearly perpendicular to the PhOH<sup>+</sup> plane. MA is oriented such that its methyl group is nearly over the center of the phenyl ring, and the ring plane-to-nitrogen distance is 2.4 Å. This ‘para’ complex is bound by 0.78 eV, relative to reactants. There is an analogous complex where the nitrogen lone pair is pointing roughly at the ortho carbon atom, at a distance of 2.3 Å, and again the MA is oriented so that its methyl group is over the ring center. This complex is bound by 0.73 eV with respect to reactants. We also examined the effect of rotating the MA moiety in the ‘ortho’ complex so that its methyl group was positioned roughly equidistant between the ortho and meta hydrogen atoms, rather than over the ring center. This geometry also optimized to a stable structure, bound by 0.73 eV with respect to reactants.

There are several points of interest in the *ab initio* results with respect to the reaction mechanism. The most stable complex by over a factor of 2 is PhO–HMA<sup>+</sup>, bound by a hydrogen bond. The PhOH<sup>+</sup>–MA→PhO–HMA<sup>+</sup> rearrangement is barrierless and energetically downhill, and there is no reason to expect a bottleneck for PhO–HMA<sup>+</sup> decomposition into the HMA<sup>+</sup>+PhO products. Taken together, these results indicate that for reactants in the hydrogen-bonding

PhOH<sup>+</sup>–MA geometry, there is a facile pathway to the observed proton transfer products. There are also at least three, and probably more, ‘ring-coordination’ complexes with binding energies in the 0.75 eV range. We have not attempted to locate transition states for interconversion between different ring-coordination complexes, but for the high internal energies generated by collisional preparation, it is almost certain that interconversion is facile. Another point of interest is that the hydrogen-bonded, and nonhydrogen-bonded complexes found for PhOH<sup>+</sup>–MA are similar in both structure and binding energy, to analogous complexes found for PhOH<sup>+</sup>-ammonia.<sup>32</sup>

Further insight into the types of complexes important in the reaction can be gotten from RRKM analysis<sup>33</sup> of the lifetimes to be expected for the *ab initio* complexes. Energetics, vibrational frequencies, and rotational constants from our *ab initio* calculations were used for the complexes. Orbiting transition states<sup>34</sup> were assumed for decomposition to reactants or products, using equipartition into all active modes to estimate the recoil velocity for the centrifugal barrier calculation. The maximum orbital angular momentum available in the decomposition was estimated from the magnitude of the capture cross section and varies from  $\sim 200 \hbar$  at low  $E_{\text{collision}}$  to  $\sim 425 \hbar$  at 2 eV.

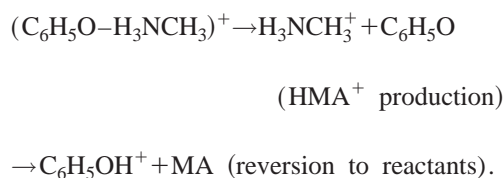
The hydrogen-bonded PhO–HMA<sup>+</sup> complex can decompose either to PhO+HMA<sup>+</sup> products or back to reactants, and both channels are included in the RRKM analysis. RRKM lifetimes for PhO–HMA<sup>+</sup> range from hundreds of picoseconds at  $E_{\text{collision}}=0.1$  eV to  $\sim 3$  ps at  $E_{\text{collision}}=1$  eV. The experimental velocity distributions suggest that  $\tau_{\text{complex}} \gtrsim 1$  ps for  $E_{\text{collision}} \leq 1$  eV, consistent with the RRKM analysis. For  $E_{\text{collision}}=2.2$  eV, the osculating complex fit to experiment gives  $\tau_{\text{complex}} \leq 290$  fs, while the RRKM lifetime is 150–190 fs. The agreement between calculation and experiment indicates that a complex with properties similar to those of the hydrogen-bonded PhO–HMA<sup>+</sup> *ab initio* complex must be responsible for the observed lifetime. Indeed, given that the PhO–HMA<sup>+</sup> complex is quite product like, it is intuitive that the reactive collisions must pass through this geometry.

RRKM analysis indicates that the nonhydrogen-bonded, ring-coordination complexes are too weakly bound to account for the lifetimes inferred from the velocity distributions. Even for the most strongly bound para complex, the lifetime is less than 100 fs at  $E_{\text{collision}} \approx 1$  eV, where experiment suggests a lifetime greater than one picosecond. It should be noted that this RRKM analysis only includes decay back to reactants, whereas, it is likely that there is also a substantial rate for decay to products and for conversion to other ring-coordination complexes. We are not able to include these channels in the analysis because the transition states are unknown, nonetheless, it is possible to estimate the effects. Interconversion between ring-coordinated complexes is probably facile, and effectively increases the total density of states associated with the set of complexes, increasing the lifetime by a factor roughly equal to the number of complexes in the set. The most likely factor is between 4 and 6. On the other hand, including the exoergic ‘decay to products’ channel will decrease the RRKM lifetime. Our conclu-

sion is that the ring-coordinated complexes have lifetimes long enough to significantly affect the collision dynamics, but almost certainly too short to account for the experimental collision times, except perhaps at our lowest energies.

The picture that emerges is that increasing collision energy inhibits reactivity in two ways. The major effect is simply that the impact parameter range over which reactants can be captured into an intimate collision decreases with increasing collision energy. Even when this effect is normalized out, however, there is a slow decrease in proton transfer efficiency with increasing energy (e.g., for the ground state, efficiency drops from  $\sim 71\%$  to  $\sim 50\%$ ). Given that the velocity distributions and RRKM analysis indicate that the  $\text{PhO-HMA}^+$  complex lifetime also decreases with increasing energy, one might think that there is a causal connection between  $\text{PhO-HMA}^+$  lifetime and  $\text{HMA}^+$  formation efficiency.

Such a connection is ruled-out by RRKM analysis of the branching for decomposition of the  $\text{PhO-HMA}^+$  complex:



The relative RRKM rates for these two channels indicate that once the  $\text{PhO-HMA}^+$  complex forms, it nearly always ( $>99\%$ ) goes on to the exoergic  $\text{HMA}^+ + \text{PhO}$  product channel, even at our highest collision energies. The implication is that the observed collisional or vibrational inhibition of  $\text{HMA}^+$  production must result from reduced efficiency for  $\text{PhO-HMA}^+$  complex formation, rather than some behavior following complex formation.

Further evidence supporting the idea that the rate-limiting step is prior to formation of  $\text{PhO-HMA}^+$  comes from the observed mode-specificity of the vibrational effects. For such a strongly bound complex, where bonding is substantially altered from that of the reactants, the initial reactant vibrational mode is scrambled during complex formation. In that case, mode specific behavior can only occur if the rate-limiting step is prior to complex formation.

Though  $\text{PhO-HMA}^+$  complex lifetime cannot be the mechanism for collisional and vibrational inhibition, collision time scale is important. There are two related effects. Proton transfer requires that the  $\text{PhOH}^+$  proton be attacked by the MA nitrogen lone pair. At low-collision energies, the time scale for reactant approach is relatively slow, possibly allowing time for re-orientation of the reactants into favorable geometry (time to traverse  $5 \text{ \AA}$  at  $0.2 \text{ eV}$  is  $\sim 400 \text{ fs}$ ). The interaction between the  $\text{PhOH}^+$  charge and the methylamine dipole moment ( $1.47 \text{ Debye}$ , pointing away from the  $N$ -lone pair) favors orienting methylamine so that the  $N$  lone pair is directed toward  $\text{PhOH}^+$ . In addition, interaction of the methylamine dipole with that of  $\text{PhOH}^+$  ( $1.46 \text{ Debye}$ , pointing approximately from O to H) will favor orienting  $\text{PhOH}^+$  in the correct geometry for hydrogen bond formation and proton transfer. As the collision energy is raised, the approach time decreases, thus decreasing the chance for re-

orientation. This argument might partly explain the slow decline in PT efficiency with increasing  $E_{\text{collision}}$ , but cannot explain the vibrational inhibition.

In addition to possible re-orientation in the approach channel, there is the possibility of forming a nonhydrogen-bonded precursor complex that might provide reactants with additional time to find the reactive geometry. As noted above, there are several ring-coordinated complexes with lifetimes dropping from tens of picoseconds at low-collision energies to subpicosecond for  $E_{\text{collision}} > 1 \text{ eV}$ . Collisions in such geometries will be common simply because the ring is a large target. Given the  $\sim 0.75 \text{ eV}$  binding energies in the ring-coordinated geometries, a substantial fraction of collisions must trap into such complexes, at least for low-collision energies. If a transition state exists that allows ring-coordinated complexes to rearrange into a hydrogen-bonded geometry where proton transfer can occur, then they provide an additional route to products. Unfortunately, the reaction coordinate separating a geometry like the para complex from the hydrogen-bonded geometry is almost certainly rather complicated, with multiple minima and transition states. The nature of the rate limiting transition state(s) is unclear, and we have not been successful in locating it by *ab initio* calculations, either for  $[\text{PhOH-MA}]^+$  or for the simpler but analogous  $[\text{PhOH-NH}_3]^+$  system. Nonetheless, it is clear that the longer the collision time, the more likely a nascent precursor complex is to rearrange into the reactive geometry. In this scenario, we would expect both collision energy and vibrational energy to reduce the precursor lifetime, and thus decrease reactivity. This precursor mechanism seems to be the best explanation for the mode-independent inhibition observed at low energies.

Neither re-orientation nor a precursor complex mechanism can explain the anomalously large inhibition from vibration at high-collision energies. At low-collision energies, inhibition depends only on total energy. The slope of the energy dependence is  $\sim 320\%$  inhibition *per* electron volt of either collision or vibrational energy in the  $E_{\text{total}}$  range around  $0.1\text{--}0.2 \text{ eV}$ . As just discussed, such nonspecific inhibition is consistent with a scenario where a weakly bound precursor complex mediates transition to the hydrogen-bonded geometry where proton transfer occurs.

For collision energies greater than  $\sim 1 \text{ eV}$ , the reaction cross section depends weakly on  $E_{\text{collision}}$ , while vibrational inhibition actually becomes slightly stronger at high energies. In the  $E_{\text{collision}}$  range between  $1$  and  $2 \text{ eV}$ , the inhibitory effect of additional collision energy is only  $\sim 13\%/eV$ , averaged over the three reactant vibrational states. Conversely, the effect of  $\nu_{6a}$  excitation is  $\sim 270\%/eV$ , averaged over the  $1$  to  $2 \text{ eV}$  collision energy range, and the averaged effect of  $\nu_{12}$  is  $\sim 330\%/eV$ . This continuing large and mode-specific effect of vibrational excitation at high total energies is difficult to explain. Both vibrations are  $x$ -sensitive, in-plane, phenyl ring distortions (top of Fig. 1), and the vibrational energies are only a few percent of  $E_{\text{total}}$  at our highest energy. Neither mode involves OH stretching, although there is significant motion of the OH group relative to the ring. In  $\nu_{6a}$  the COH moiety moves as a unit, while in  $\nu_{12}$  there is significant CO stretching character.

The only example allowing comparison of vibrational effects in a similar system is the reaction of  $\text{PhOH}^+$  with  $\text{ND}_3$ .<sup>22,32</sup> The dominant reaction in that system is  $H/D$  exchange, producing  $\text{PhOD}^+ + \text{ND}_2\text{H}$ . For  $H/D$  exchange there is substantial *enhancement* from both  $\nu_{6a}$  and  $\nu_{12}$  excitation at low-total energies, dying out as  $E_{\text{collision}}$  increases, with little vibrational effect above 0.5 eV. This loss of vibrational effect at high  $E_{\text{total}}$  is typical of polyatomic atom-transfer reactions we have studied<sup>5–15,35,36</sup> and is not surprising—at high energies the vibrational energy is a negligible fraction of  $E_{\text{total}}$ , and the collision outcome is largely determined by approach geometry.

Proton transfer to ammonia is also observed, but is a minor channel because it is endoergic by  $\sim 0.2$  eV. The vibrational effects are quite interesting, however. Vibration has little effect in the threshold region, where one might expect enhancement from vibrational energy. At  $E_{\text{collision}}$  above  $\sim 0.5$  eV there is inhibition from vibration excitation, of similar proportion to that observed in the  $\text{PhOH}^+ + \text{MA}$  system. Tentatively, therefore, it seems that inhibition by in-plane ring vibration is a common feature in high  $E_{\text{collision}}$  proton transfer from  $\text{PhOH}^+$  to  $\text{NH}_2\text{X}$  ( $\text{X}=\text{H}, \text{CH}_3$ ), even though the PT energetics and efficiency are very different in the two systems. The origin of the surprising effect is unclear.

One scenario we considered is that vibration might change the charge distribution, thus somehow decreasing reactivity. To test this notion, GAUSSIAN 98 calculations were repeated for  $\text{PhOH}^+$  distorted from its equilibrium geometry in both directions along both the  $\nu_{6a}$  and  $\nu_{12}$  normal coordinates. Distortions of 40% of the normal mode vectors reported by GAUSSIAN 98 were used. Judging from the energies at these distorted geometries ( $\sim 0.2$  to  $\sim 1$  eV above the equilibrium geometry), the distortions are substantially larger than the classical vibrational amplitudes, and therefore, should overestimate any charge redistribution effects. For  $\text{PhOH}^+$  at its equilibrium geometry, the Mulliken charge distribution is as follows:  $H_{\text{OH}}=0.47$ ,  $\text{O}=-0.50$ ,  $\text{C}_1=0.39$ ,  $\text{C}_2=-0.10$ ,  $\text{C}_3=-0.11$ ,  $\text{C}_4=-0.07$ ,  $\text{C}_5=-0.11$ ,  $\text{C}_6=-0.14$ , with all other H atoms between 0.22 and 0.24.  $\text{C}_1$  is the carbon atom where OH is attached,  $\text{C}_2$ – $\text{C}_6$  are clockwise from  $\text{C}_1$  as in Fig. 1. As expected, the OH bond is polar, and there is significant polarization of the CO bond as well. The charge distribution changes very little with vibrational distortion, however. The maximum change in Mulliken charge on an atom is 0.03, and the rms (root-mean-square) change is only 0.014. The changes in atomic charge within the COH moiety are only 2%–4% of the equilibrium values. Given that the distortions imposed were exaggerated, it seems unlikely that the vibration-induced charge redistribution is mechanistically significant.

At high energies, one normally thinks of dynamical, rather than energetic influences to explain observed behavior of reactions. It is useful to consider time scales. The classical period of the vibrations is  $\sim 65$  and  $\sim 40$  fs for  $\nu_{6a}$  and  $\nu_{12}$ , respectively. At  $E_{\text{collision}}=1$  eV, these times correspond to relative motion of the reactants of 1.8 and 1.1 Å, respectively. These distances are on the order of a bond length, i.e., the vibrational time scale corresponds to relative motion in

the range expected to be critical in determining dynamics. It seems likely, therefore, that the vibrational effect results from some coupling between the OH vibrational motion and relative motion with respect to methylamine. It is not at all obvious how this coupling reduces the proton transfer efficiency. One possibility is something that might be referred to as dynamical steric hindrance. In both the  $\nu_{6a}$  and  $\nu_{12}$  vibrations, the distance between the hydroxyl proton and the nearest ring hydrogen is modulated by a few tenths of an angstrom. On average, of course, the distance is unaffected, but it may be that approach from some orientations is impeded by the oscillating distance, such that there is a net inhibition. We will attempt to examine the effects of non- $x$ -sensitive vibrations on this reaction, in order to shed additional light on the origin of these unexpected vibrational effects.

#### IV. CONCLUSIONS

The proton transfer reaction of  $\text{PhOH}^+$  with methylamine proceeds with  $\sim 75\%$  efficiency for low  $E_{\text{collision}}$  and no  $\text{PhOH}^+$  vibrational excitation. PT is found to go by a long-lived hydrogen-bonded complex at low energies, with collision time and extent of energy redistribution decreasing markedly with increasing energy in the  $< 2$  eV range. Both vibration and  $E_{\text{collision}}$  inhibit proton transfer with similar efficacy at low  $E_{\text{collision}}$ , and this effect is tentatively attributed to reduction in collision time scale due to decreased lifetime of a weakly bound precursor complex. At high  $E_{\text{collision}}$ , collision energy has little effect on reaction efficiency, while vibrational state continues to have a significant, and mode-specific effect. The effect is similar to that observed in  $\text{PhOH}^+ + \text{NH}_3$  proton transfer, and the origin is proposed to be a dynamical effect, rather than some effect of vibrational energy or vibrational distortion of the electron density.

- <sup>1</sup>S. L. Anderson, Adv. Chem. Phys. **82**, 177 (1992).
- <sup>2</sup>R. D. Guettler, G. C. Jones, Jr., L. A. Posey, and R. N. Zare, Science **266**(5183), 259 (1994).
- <sup>3</sup>L. A. Posey, R. D. Guettler, N. J. Kirchner, and R. N. Zare, J. Chem. Phys. **101**, 3772 (1994).
- <sup>4</sup>L. A. Posey, R. D. Guettler, and R. N. Zare, Proc. SPIE-Int. Soc. Opt. Eng. **1638**, 431 (1992).
- <sup>5</sup>B. Yang, Y. H. Chiu, H. Fu, and S. L. Anderson, J. Chem. Phys. **95**, 3275 (1991).
- <sup>6</sup>B. Yang, Y. H. Chiu, and S. L. Anderson, J. Chem. Phys. **94**, 6459 (1991).
- <sup>7</sup>Y.-h. Chiu, H. Fu, J.-t. Huang, and S. L. Anderson, J. Chem. Phys. **105**, 3089 (1996).
- <sup>8</sup>Y.-h. Chiu, H. Fu, J.-t. Huang, and S. L. Anderson, J. Chem. Phys. **102**, 1188 (1995).
- <sup>9</sup>T. M. Orlando, B. Yang, and S. L. Anderson, J. Chem. Phys. **90**, 1577 (1989).
- <sup>10</sup>T. M. Orlando, B. Yang, Y. H. Chiu, and S. L. Anderson, J. Chem. Phys. **92**, 7356 (1990).
- <sup>11</sup>Y.-h. Chiu, B. Yang, H. Fu, S. L. Anderson, M. Schweizer, and D. Gerlich, J. Chem. Phys. **96**, 5781 (1992).
- <sup>12</sup>Y.-h. Chiu, H. Fu, J.-t. Huang, and S. L. Anderson, J. Chem. Phys. **101**, 5410 (1994).
- <sup>13</sup>Y.-h. Chiu, H. Fu, J.-t. Huang, and S. L. Anderson, J. Chem. Phys. **102**, 1199 (1995).
- <sup>14</sup>J. Qian, H. Fu, and S. L. Anderson, J. Phys. Chem. **101**, 6504 (1997).
- <sup>15</sup>H. Fu, J. Qian, R. J. Green, and S. L. Anderson, J. Chem. Phys. **108**, 2395 (1998).
- <sup>16</sup>H. Palm, D. Berthomieu, C. Metayer-Zeitoun, C. Alcaez, and O. Dutuit, Proc. SASP'94, 180 (1994).
- <sup>17</sup>C. Metayer-Zeitoun, C. Alcaez, S. L. Anderson, H. Palm, and O. Dutuit, J. Phys. Chem. **99**, 15523 (1995).

- <sup>18</sup>I. Koyano and K. Tanaka, *J. Chem. Phys.* **72**(9), 4858 (1980).
- <sup>19</sup>I. Koyano and K. Tanaka, *Adv. Chem. Phys.* **82**, 263 (1992).
- <sup>20</sup>Z. Herman, K. Tanaka, T. Kato, and I. Koyano, *J. Chem. Phys.* **85**(10), 5705 (1986).
- <sup>21</sup>L. Zhu and P. Johnson, *J. Chem. Phys.* **94**, 5769 (1991).
- <sup>22</sup>H.-T. Kim, R. J. Green, J. Qian, and S. L. Anderson, *J. Chem. Phys.* (to be published).
- <sup>23</sup>M. Yi and S. Scheiner, *Chem. Phys. Lett.* **262**, 567 (1996).
- <sup>24</sup>S. G. Lias, J. F. Liebman, and R. D. Levin, *J. Phys. Chem. Ref. Data* **13**, 695 (1984).
- <sup>25</sup>S. G. Lias, J. E. Bartmess, J. F. Liebman, J. L. Holmes, and R. D. Levin, *J. Phys. Chem. Ref. Data* **17**, 1 (1988).
- <sup>26</sup>S. L. Anderson, L. Goodman, K. Krogh-Jespersen, A. G. Ozkabak, R. N. Zare, and C.-f. Zheng, *J. Chem. Phys.* **82**, 5329 (1985).
- <sup>27</sup>D. Gerlich, *Adv. Chem. Phys.* **82**, 1 (1992).
- <sup>28</sup>GAUSSIAN 98, M. J. Frisch, G. W. Trucks, H. B. Schlegel, G. E. Scuseria, M. A. Robb, J. R. Cheeseman, V. G. Zakrzewski, J. A. Montgomery, R. E. Stratmann, J. C. Burant, S. Dapprich, J. M. Millam, A. D. Daniels, K. N. Kudin, M. C. Strain, O. Farkas, J. Tomasi, V. Barone, M. Cossi, R. Cammi, B. Mennucci, C. Pomelli, C. Adamo, S. Clifford, J. Ochterski, G. A. Peterson, P. Y. Ayala, Q. Cui, K. Morokuma, D. K. Malick, A. D. Rabuck, K. Raghavachari, J. B. Foresman, J. Cioslowski, J. V. Ortiz, B. B. Stefanov, G. Liu, A. Liashenko, P. Piskorz, I. Komaromi, R. Gomperts, R. L. Martin, D. J. Fox, T. Keith, M. A. Al-Laham, C. Y. Peng, A. Nanayakkara, C. Gonzalez, M. Challacombe, P. M. W. Gill, B. G. Johnson, W. Chen, M. W. Wong, J. L. Andres, M. Head-Gordon, E. S. Replogle, and J. A. Pople (Gaussian, Inc., Pittsburgh, PA, 1998).
- <sup>29</sup>L. Laaksonen, 1.31 ed. (available at <http://laaksonen.csc.fi/gopenmol/gopenmol.html>, Espoo, Finland, 1999).
- <sup>30</sup>J. Troe, *Chem. Phys. Lett.* **122**, 425 (1985).
- <sup>31</sup>G. A. Fisk, J. D. McDonald, and D. R. Herschbach, *Discuss. Faraday Soc.* **44**, 228 (1967).
- <sup>32</sup>R. J. Green, H.-T. Kim, J. Qian, and S. L. Anderson (in preparation).
- <sup>33</sup>L. Zhu and W. L. Hase (*Quant. Chem. Prog. Exchange*, QCPE 644).
- <sup>34</sup>M. T. Rodgers, K. M. Ervin, and P. B. Armentrout, *J. Chem. Phys.* **106**, 4419 (1997).
- <sup>35</sup>J. Qian, R. J. Green, and S. L. Anderson, *J. Chem. Phys.* **108**, 7173 (1998).
- <sup>36</sup>S. L. Anderson, *Acc. Chem. Res.* **30**, 28 (1997).